Surface Characterization of Polyester Fibers

GUNILLA GILLBERG and DAVID KEMP, *Celanese Research Company, Summit, New Jersey 07901*

Synopsis

Fibers made from poly(ethylene terephthalate) (PET) are characterized by a hydrophobic surface with low reactivity. Modifications of the PET surface to render a higher degree of hydrophilicity and reactivity are therefore common. The modification often involves a surface layer of only a few nanometers thickness. The relatively low fraction of the modified surface layer and the fact that it is generally an organic modification on a thin curved organic substrate presents difficulties in surface analyses. Surface characterization is, however, of high importance in the evaluation of the degree and durability of a given surface modification. The paper will discuss the possibilities and the limits of using wettability studies according to the Wilhelmy method to evaluate the degree of surface modification and its permanence. Comparison between internal and external reflection Fourier-transform infrared spectroscopy will be made. The use of electron spectroscopy for chemical analysis, secondary ion mass spectrometry, laser microprobe mass analysis, and microprobe molecular optics laser examiner will be illustrated. Data will be presented from studies of model yarns and films coated with D-417 dip.

INTRODUCTION

Fibers made from poly(ethylene terephthalate) (PET) are characterized by a hydrophobic surface with low reactivity. Modifications of the PET surface to render a higher degree of hydrophilicity and reactivity are therefore common. The modifications often involve a surface layer of only a few nanometers thickness. The comparatively low fraction of the modified surface layer and the fact that it is generally an organic modification on a small curved organic substrate presents difficulties in the evaluation of the degree and durability of a given surface modification. Considerable efforts have been made to develop techniques for the characterization of fiber surfaces.[1]

Two different approaches have been pursued to improve the adhesion of polyester cord to the traditional cord adhesive, the resorcinol-formaldehyde-latex (RFL) dip. (A cord consists of two to three plies of yarns twisted together.) The oldest method (so-called double-dip systems) involves treatment of the cord surface with an intermediate adhesive layer and then with the RFL-dip. DuPont's D-417 dip has been one of the most popular intermediate adhesives in the double-dip system in the past. This dip consists of a phenol-blocked methylene-bisphenylene diisocyanate (Hylene MP) and a glycerol epoxy resin (Epon 812) as active components, a wetting agent and water. The unblocking of the isocyanate takes place first, after the water has evaporated, and the major reaction occurs between the isocyanate and the epoxy to form a polyurethane.[2] Spin finish components such as sulfated esters and fatty acids have been shown to interfere with the unblocking reaction.[2]

The other systems are the so-called single dips where the most poular ones utilize adhesive activated polyester yarns. The adhesive activation involves a

Journal of Applied Polymer Science, Vol. 26, 2023–2051 (1981)
 CCC 0021-8995/81/062023-29$02.90

surface modification of the PET fibers during the yarn manufacturing process, which leads to a very satisfactory adhesion to a standard RFL dip. In general, the tire producers prefer the single dip systems due to much lower manufacturing cost and excellent tire performance. Fiber Industries is one of the leading producers of adhesive activated PET tire yarn in the U.S.A. An example of one of their adhesive activated tire yarns is T-811. T-800 is a nonadhesive activated tire yarn.

The D-417 double-dip system gives adhesion superior to the adhesive activated tire yarns in laboratory adhesion tests. However, the adhesive activated tire yarns yield superior tire performance. The better static adhesion can be a result of D-417 giving a better bonding to PET and RFL but can also reflect the fact that coating the cord with the adhesive gives better surface distribution for both the intermediate adhesive and the RFL dip. We thought it would be interesting to see if it was possible to distinguish between the importance of the chemistry and of the configuration by topcoating yarn with the D-417 dip. This yarn would also be very suitable for evaluating the feasibility of various surface characterization techniques since the formed urethane, the nitrogen in the isocyanate molecule, and the chlorine in the glycerol epoxy should give spectra distinctly different from the PET in various spectroscopic techniques.

Adhesion testing of the D-417 coated yarn did not give the adhesion of the coated cord. Questions which arise are: Was the difference due to the different geometric configuration? Did the thinner films, the higher relative concentration of spin finish components, and the higher curvature of the coated yarn interfere with the polyurethane reaction? Did we obtain an even coating of D-417 on the top-coated yarn?

The techniques we used were optical and scanning electron microscopy (SEM), wettability, Fourier-transform infrared spectroscopy (FTIR), Raman microspectroscopy (MOLE), laser microprobe mass analysis (LAMMA), secondary ion mass spectrometry (SIMS), and electron spectroscopy for chemical analysis (ESCA).

MICROSCOPY

An imaging of the surface with optical or scanning electron microscopy is an essential starting point of surface analysis. Optical microscopy has the advantages of very little sample preparation, plus the ability to record color, and birefringence. It is also comparatively easy to scan large surface areas. The limits are the low resolution (on the order of 1 μm) and, especially at high magnifications, the limited depth of focus which is especially disadvantageous in the case of the curved fiber surfaces. Only gross distributions or topographical variations can thus be observed. A finish level of 1%, when evenly distributed on a fiber with diameter of 20 μm will have an average thickness of 70 nm, i.e., less than the wave length of light. Optical microscopy will thus not be able to show the presence of evenly distributed finishes.

The scanning electron microscope has a resolution of ca. 100 Å with a great depth of focus. The low electrical conductivity of polymeric fibers makes coating of the fibers with a thin conductive layer necessary to avoid charging, which would prevent good imaging from being obtained under standard conditions. The use of low accelerating voltages (1 keV), low magnification, and TV scan which re-

quires only short exposure time, allows studies without coating.[3] However, the high vacuum of the electron microscope will cause evaporation of volatile material. The same problem arises with the deposition of conductive metal coatings which is also performed under vacuum. The more laborious replication technique[4] should always be performed as a control to ensure that the metal depositions do not cause image artifacts.[3]

The ability of the SEM to resolve unevenly distributed finishes on fiber surfaces is well illustrated in Figures 1(A) and 1(B). The finish is generally distributed as small globules of sizes from approximately 0.1 μm and up. A string of finish (arrow), formed in an interstice originally existing between two filaments, is also seen. The SEM cannot discern if a thin finish film also exists

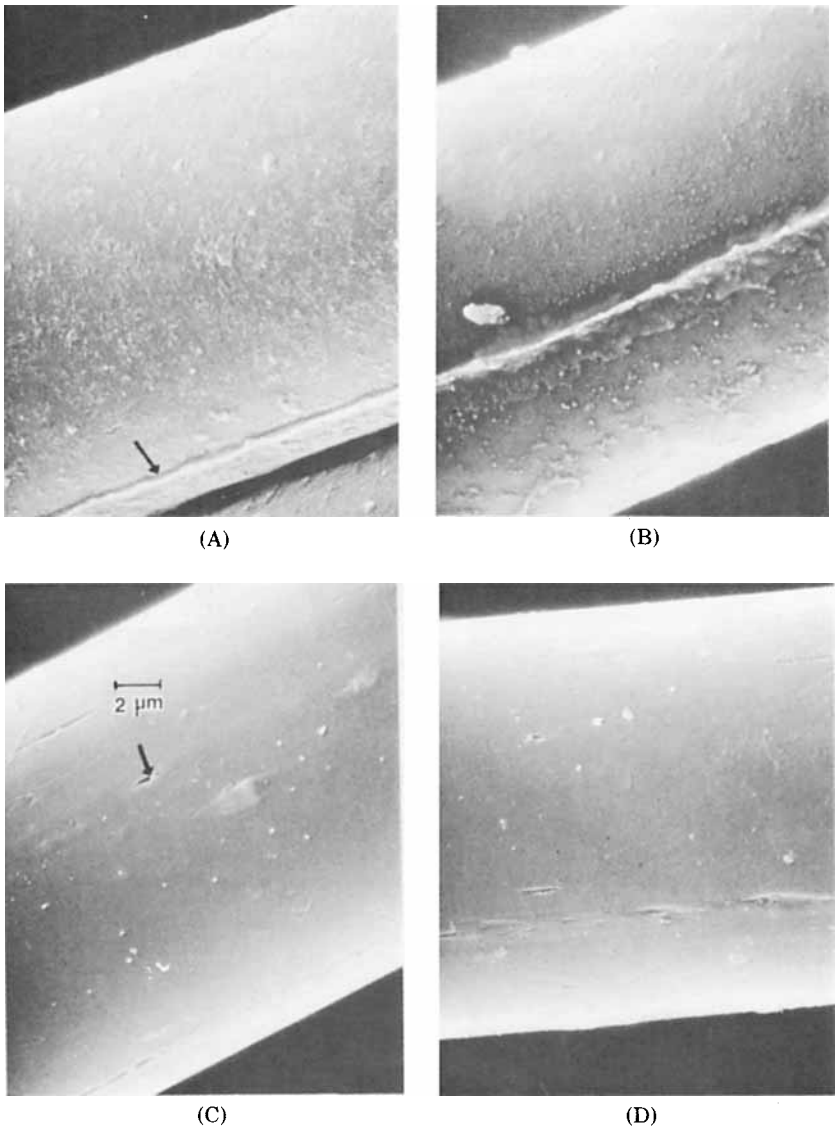

(A) (B)

(C) (D)

Fig. 1. SEM photomicrographs of TiO_2 filled polyester fibers with original spin finish present on the surface at 5000× (A, B) and after 5 min ultrasonic methanol cleaning at 5000× (C, D).

between the globules. Cleaning the fibers with methanol removes the finish and irregularities in the surface can then be seen [Figs. 1(C) and 1(D)]. Titanium dioxide particles are visible in slots on the fiber surface [arrow, Fig. 1(C)].

Our model yarn, the tire yarn coated with DuPont's D-417 dip and heat cured, was also investigated by SEM and the results are given in Figure 2. It is evident from Figure 2(A) that the coating is unevenly distributed across the yarn bundle with an excess bridging some fibers. Cleaning the fibers with methanol removes a considerable amount of the original coating but some material still remains on the surface [Fig. 2(D)]. This material is most probably reaction products of the D-417 system, since finish lubricants are removed during the cleaning operation (Fig. 1). For comparison, SEM photomicrographs were also taken of a cord coated with D-417 after an ultrasonic methanol cleaning (Fig. 3). The high magnifications show that a much thicker and almost continuous surface coating exists on the fiber surfaces in the case of cord treatment and that this coating resists ultrasonic cleaning.

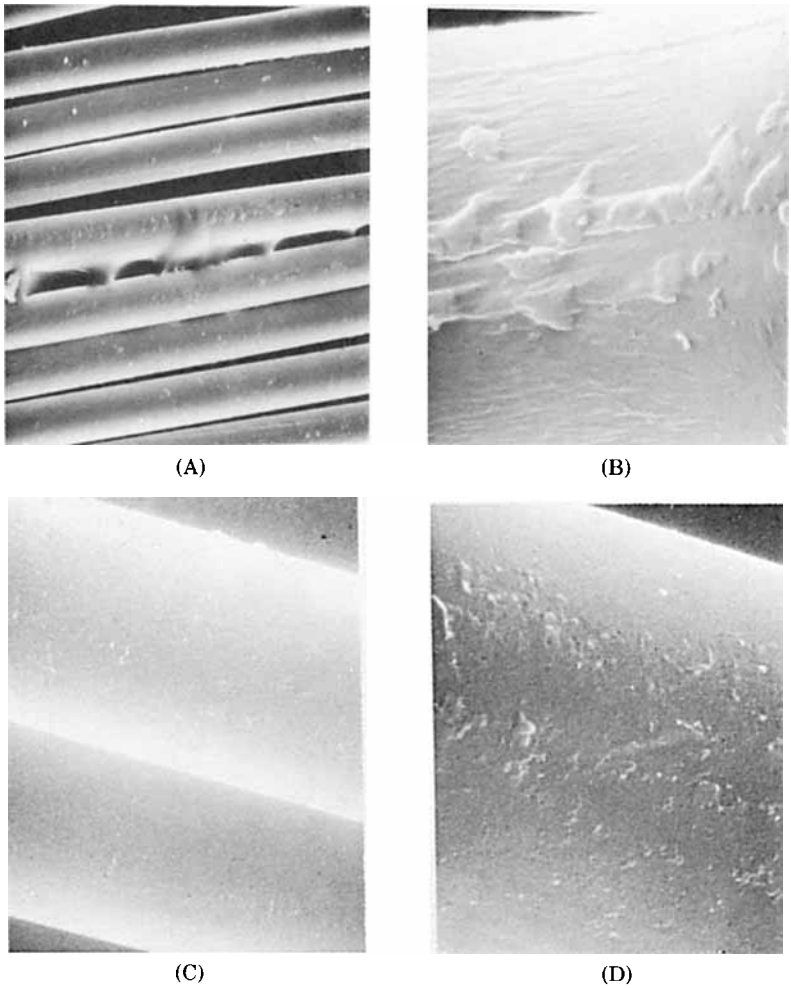

Fig. 2. SEM photomicrographs of tire yarn T-811 top-coated with 1% of DuPont's D-417 dip and heat cured. Fibers as received at 100× (A) and 5000× (B) and after 5 min ultrasonic methanol cleaning at 2000× (C) and 5000× (D).

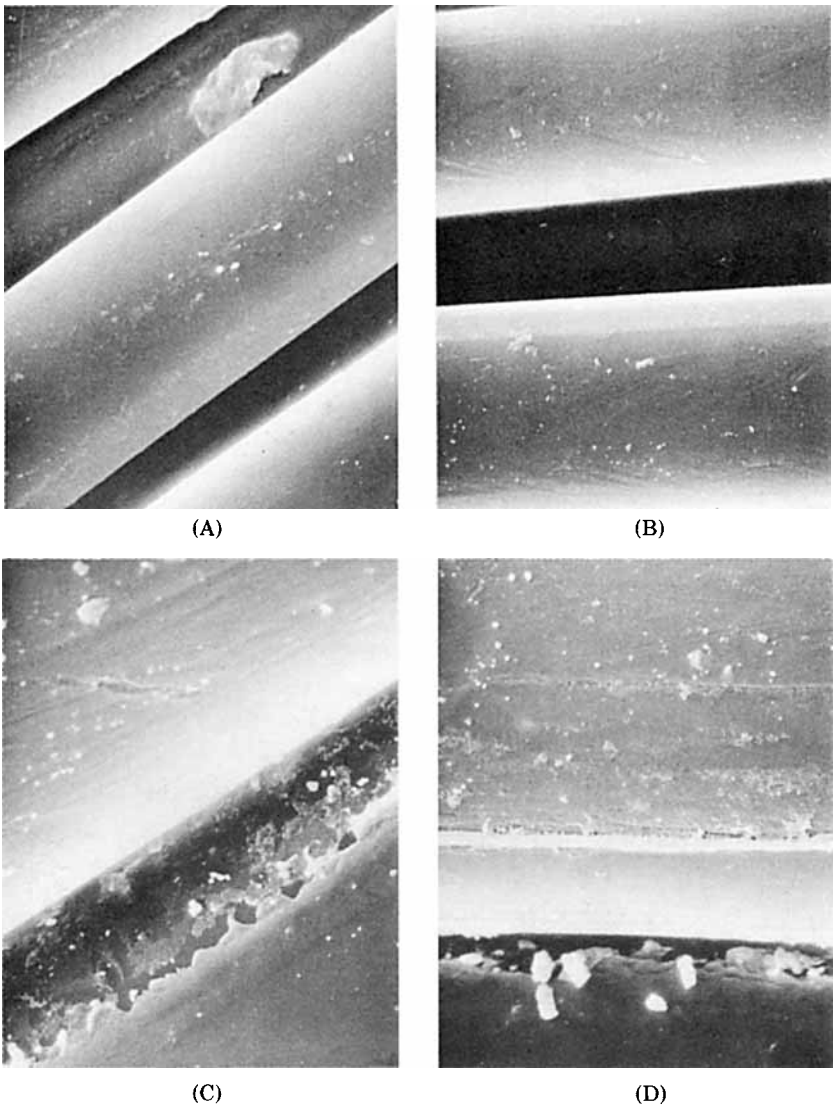

Fig. 3. SEM photomicrographs of cords coated with D-417 dip heat treated and later 5 min ultrasonically methanol cleaned at 2000× (A, C) and at 5000× (B, D).

SEM investigations are thus an excellent tool to reveal the presence of unevenly distributed material on a fiber surface. The electrons which penetrate the solid, cause ionization and thereby x-ray fluorescence. Most modern SEM instruments have equipment for energy dispersive x-ray analysis. Surface mapping is, however, rarely successful for very thin coatings due to low signal intensities.

WETTABILITY

There is no direct method of measuring the surface energy of a solid surface. Several indirect methods to estimate the surface energy have been used such as extrapolation of data for melts, use of a simplified solution to the Fowler equation,

polarizabilities and diamagnetic susceptibilities, estimates from group parachors, and contact angle measurements.[4–6] The most popular method is probably contact angle measurements with well defined liquids. Various theories have been used for estimating the surface energy from contact angle data. Good and Girifalco have proposed the use of the following expression:[7,8]

$$\gamma_s = [\gamma_L(1 + \cos\theta) + \pi_e]^2/4\phi^2\gamma_L \quad (1)$$

where γ_s is the surface energy of the solid, γ_L is the surface tension of the liquid, θ is the equilibrium contact angle, π_e is the equilibrium spreading pressure, and ϕ is an interaction parameter. π_e is generally thought to be negligible if $\theta > 0$, and in that case

$$\gamma_s = [\gamma_L\ (1 + \cos\theta)^2]/4\phi^2 \quad (2)$$

The interaction parameter ϕ can be calculated if composition, structure, and molecular properties of the solid and liquid are known.[8]

Fowkes[9] showed that a further understanding was obtained if the surface energy was divided into components due to dispersion, polar, and hydrogen bonding. The attraction forces at an interface could thus be attributed to the interaction of matched components. The dispersive attraction was calculated as the geometric mean of the dispersion forces.

Owens and Wendt[10] and Kaelble[11] developed this theory further by also assuming that the polar attraction forces which included the hydrogen bonding, could be described by a geometric mean expression. Assuming the film pressure π_e is negligible, the work of adhesion between a liquid and a solid could thus be described by

$$W_{\text{ADH}} = \gamma_L\ (1 + \cos\theta) \simeq 2\ (\gamma_L^d\gamma_S^d)^{1/2} + 2(\gamma_L^p\gamma_S^p)^{1/2} \quad (3)$$

where the superscripts d and p denote dispersive and polar, respectively. Introduction of $\alpha^2 = \gamma^d$ and $\beta^2 = \gamma^p$ and rearrangement of eq. (3) gives

$$[\gamma_L\ (1 + \cos\theta)]/2\alpha_L = \alpha_S + \beta_S\ (\beta_L/\alpha_L) \quad (4)$$

Tables of values of α_L and β_L for several liquids have been published.[11,12] By measuring the contact angle for several liquids, α_S and β_S (i.e., γ_S^d and γ_S^p) can be determined graphically or by determinant calculations.[12] Surface energies of the most common polymers have been estimated according to this method.[12]

Wu[9,10,13,14] found better agreement in his measurements if he used a harmonic-mean equation as a combining rule for the polar and dispersive forces, respectively.

Fowkes[15–17] has called attention to the mistake of assuming the polar component to be constant and independent of the system under consideration. Besides dipole interactions, the polar component also includes acid-base (donor-acceptor) interactions. (Hydrogen bonds are a special class of donor-acceptor interactions.) If the liquid and the surface are both acidic or both basic, very small polar interactions will take place compared to the case in which one of them is a donor and the other an acceptor. Fowkes[15,16] thus proposes the following expression for the work of adhesion:

$$W_{\text{ADH}} = 2(\gamma_A^d\gamma_B^d)^{1/2} - K(C_AC_b + E_AE_b) \times \frac{\text{moles of acid-base pairs}}{\text{unit area}} + W_{\text{ADH}}^p \quad (5)$$

where subscripts A and B denote acid and base, respectively, and C and E are constants according to Drago's nomenclature. Although this approach does not allow any easy estimation of the surface energy of the polymer it should give a more correct evaluation of interfacial interaction energies.

In the case of surface modification, patchy composite surfaces might result. Cassie has proposed that the equilibrium angle should be the area weighted average[8,18]

$$\cos\theta_c = Q_1 \cos\theta_1 + Q_2 \cos\theta_2 \tag{6}$$

where Q_i is the fraction of surface having a contact angle θ_i. A correct surface energy treatment of composite surface must involve the definition of dispersive, polar and donor-acceptor components for each type of surface element.

Analysis of a model heterogeneous surface, consisting of concentric rings, showed that advancing contact angles would be a good measure of the wettability of the low-energy part of the surface and receding contact angles of the high-energy part but that neither contact angle would give a reliable measure of surface coverage.[18] 10% to 90% coverage of one type of surface thus gave about the same advancing contact angle. In a more recent study, Smith and Lindberg[19] used dot test patterns on lithographic plates to create a composite surface with advancing water contact angles of about 81° and 3°, respectively, for the two surface types. This investigation showed that the experimental advancing contact angles fall within 10%–15% of the theoretical curve according to Cassie's equation. Surface coverage could thus be evaluated from the measured contact angles.

Another problem with contact angle measurements on polymers is that many of the typical organic probe liquids will dissolve or swell the surface layer of the polymer. The degree of swelling will also be dependent on the crystallinity of the polymer. A drop of methylene diiodide placed on an amorphous PET film will thus dissolve the surface layer underneath it and cause crazing (Fig. 4), while no such effect is noticeable on a crystalline PET film. This type of interaction

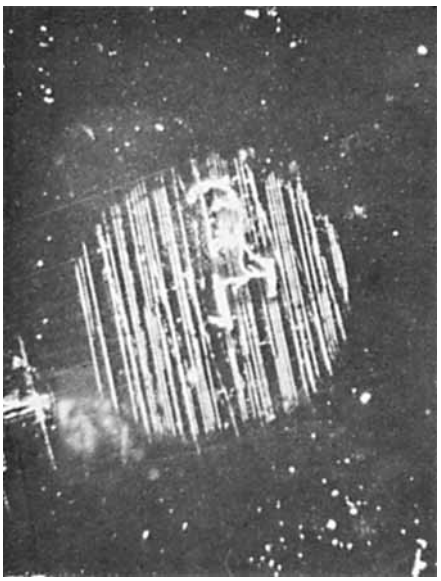

Fig. 4. Crazing caused by a drop of methylene diiodide applied onto an amorphous PET film.

has been observed for other forms of polymers and is especially troublesome in the wettability studies of fibers, where anomalous high forces are recorded (see below).

Indirect methods must be used to determine the contact angle on thin fibers.[20] The most accepted method is founded on the formula of Wilhelmy which states that the pull (F_L) exerted on a solid rod inserted into a mass of liquid is

$$F_L = P\gamma_L \cos\theta = \pi D\gamma_L \cos\theta \tag{7}$$

where $P = \pi D$ is the perimeter along the three-phase boundary line and D is the diameter of the rod (Fig. 5). On immersion in the liquid, the pulling force will be partly balanced by the buoyancy force (F_B), but in the case of fine textile fibers, the buoyancy force will be less than the general experimental noise level. The wetting force is measured by a sensitive autobalance used in the hang-down mode. The probe liquid is advanced along the dry fiber or retracted from the prewetted fiber by a motor driven elevator.[11,12,20,21]

Due to the ambiguity of the results obtained with organic probe liquids, double distilled water has been mainly used in our wetting studies to evaluate surface modifications. Our elevator, which is a micromanipulator from Hacker Instruments coupled to a B & B AC variable speed instrument motor, has a vertical speed range of 0.2–3 mm/min in either direction. The contact angles are thus measured under dynamic conditions. Earlier studies suggest that the dynamic contact angle remains equal to the static value as long as the contact line between solid, liquid, and air is moving sufficiently slowly over the solid.[22,23] Wettability studies with a finish free TiO_2-filled PET fiber (diameter 22 μm) and variation of speed show that the dynamic effects are obtained at rates above 0.8 mm/min (Fig. 6). A slight variation due to fiber variability is also seen. A rate of 0.3 mm/min was chosen as the standard rate to avoid dynamic effects. A typical trace of the wetting force as function of time and wetting mode is given in Figure 7. The trace is constructed from the 1 sec read-outs, since the autobalance used (Perkin-Elmer AD-22) only has digital output.

The digital output makes statistical analysis very convenient. An analysis of advancing wetting forces recorded for six different cleaned polypropylene fibers showed that the variation in average wetting force between fibers was sig-

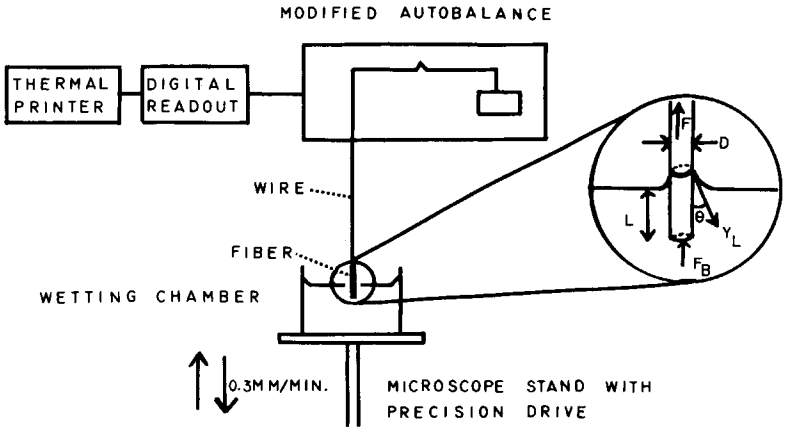

Fig. 5. Schematic picture of apparatus for measuring the wettability of fibers.

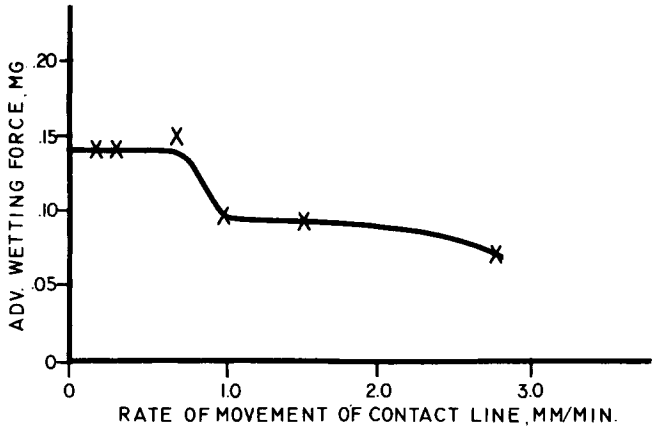

Fig. 6. Dependence of observed wetting force on rate of movement of contact line between air, water, and PET fiber.

nificantly different from that within the fibers, i.e., the long range variability is considerably larger than the short range variability. Calculations also showed that the observed differences in wetting forces would correspond to a 33% difference in fiber diameter if we assumed the fiber wettability constant. The wetting test thus indicated the presence of uneven surface deposits which had not been removed by the cleaning operation.

The fibers must be cleaned before the wetting studies are performed to remove loosely adhering surface material. This material might otherwise diffuse out from the surface during the wetting experiment and cause a local change in the surface tension of the probe liquid next to the fiber.

The variability in wetting force within and between fibers, the calculated averages of the advancing and retarding forces, and the hysteresis between these values provides information on surface heterogeneities and the extent of surface modification. A typical example is shown in Table I. Even after cleaning, the unmodified fibers show large variations which suggest that the cleaning method used was not effective in removing all spin finish components. Modifying the

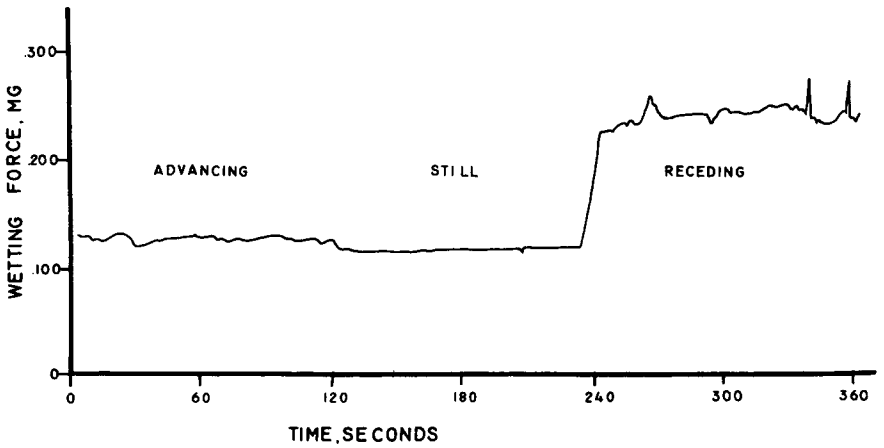

Fig. 7. Trace of wetting force as function of time for cleaned PET fiber in doubly distilled water.

TABLE I
Average Value of the Wetting Force $\bar{F}$ (mg) and the Standard Deviation S_x for Polyester Fibers After Surface Modification and Ultrasonic Methanol Cleaning Using Doubly Distilled Water as Probe Liquid

Fiber	Level of Surface Modification	Advancing		Receding	
		$\bar{F}$	S_x	$\bar{F}$	S_x
A:1	None	0.085	0.011	0.206	0.004
A:2	None	0.119	0.003	0.237	0.004
A:3	None	0.087	0.006	0.210	0.002
A:4	None	0.106	0.009	0.214	0.013
A:5	None	0.110	0.015	0.212	0.009
A:6	None	0.063	0.007	0.198	0.023
Average of averages		0.095	0.022	0.213	0.013
B:1	0.2%	0.193	0.035	0.265	0.006
B:2	0.2%	0.158	0.001	0.258	0.009
B:3	0.2%	0.174	0.044	0.267	0.046
B:4	0.2%	0.147	0.032	0.242	0.017
B:5	0.2%	0.117	0.018	0.229	0.017
B:6	0.2%	0.141	0.015	0.237	0.021
Average of averages		0.155	0.027	0.250	0.016
C:1	0.4%	0.222	0.026	0.320	0.036
C:2	0.4%	0.214	0.010	0.269	0.006
C:3	0.4%	0.229	0.006	0.278	0.015
C:4	0.4%	0.220	0.009	0.276	0.010
C:5	0.4%	0.216	0.007	0.259	0.016
C:6	0.4%	0.220	0.003	0.259	0.006
Average of averages		0.220	0.005	0.277	0.022

fiber surface with an average 0.2% hydrophilic finish yields fibers with considerably higher wetting force, i.e., a lower contact angle but also a comparatively high standard deviation. The short-range and the long-range wetting properties of these fibers vary considerably. Doubling the amount of finish gives a much more even surface treatment and the improved surface coverage is also reflected in considerably higher advancing and retarding forces, i.e., lower advancing and receding contact angles. More extensive cleanings of the fibers reduced the observed wetting forces showing that the surface treatment did not have the desired permanence.

The results of a similar investigation of the tire yarn coated with DuPont's D-417 dip (Table II) show a significantly larger variability between fibers than within fibers suggesting that the top coating with the D-417 dip resulted in an uneven distribution. Typical values for clean polyester fibers with the same diameter are an advancing force of 0.124 mg and receding force of 0.354 mg. The coated fibers show higher retarding forces, which indicates the presence of more polar groups on the surface. The advancing contact angle of water on a D-417 fiber was determined to be 60° and on clean PET to be 80°. The highest average advancing force observed for the cleaned D-417 coated yarns was 0.175 mg which corresponds to a contact angle of 71°. Using Cassie's equation (6) we estimate the D-417 coated area to be 46%; the two averages for the two cleaning methods correspond to 36% and 21% coverage, respectively. The wetting studies thus

TABLE II
Average Value of the Wetting Force, $\bar{F}$ (mg) and the Standard Deviation S_x for Polyester Yarn T-811 Coated with 1% DuPont D-417 Dip and Heat Cured Using Doubly Distilled Water as Probe Liquid

	Advancing		Receding	
Cleaning	$\bar{F}$	S_x	$\bar{F}$	S_x
5 min	0.144	0.008	0.353	0.024
ultrasonically	0.121	0.011	0.408	0.016
with methanol	0.159	0.020	0.400	0.031
	0.175	0.016	0.395	0.020
	0.169	0.016	0.399	0.008
Average of averages	0.154	0.022	0.391	0.022
24 hr soaking	0.137	0.019	0.417	0.009
in water:methanol	0.157	0.012	0.427	0.037
in a ratio of 1:1	0.109	0.010	0.400	0.013
	0.124	0.031	0.451	0.021
	0.132	0.054	0.400	0.032
Average of averages	0.132	0.017	0.420	0.022

confirm the SEM results that only partial coverage of the fiber surface has been obtained by top coating.

FOURIER-TRANSFORM INFRARED SPECTROSCOPY

Fourier-transform infrared spectroscopy (FTIR) in combination with internal reflection spectroscopy or attenuated total reflectance (ATR) has been proven to be a useful tool for surface analysis and identification of polymers.[24] The sample is squeezed against both sides of a trapezoidally shaped prism which allows the light to make multiple reflections at the prism-sample interface. Good contact between the sample and the prism is essential. While this is relatively easily obtained with film samples, fibers and yarns will inherently give a low contact area (Fig. 8). Most FTIR investigations on PET fibers are also concerned with bulk morphology evaluations (e.g., see ref. 25). Thicker coatings on fiber assemblies have been successfully identified,[26–28] while finishes at levels less than 1% have not been detected in general by the ATR technique.[26,28] This is because the penetration depth of the IR radiation in the sample medium is much larger than the average thickness of 35 nm, which 1% finish would yield on a PET fiber with a 10 μm diameter. The penetration depth is defined as

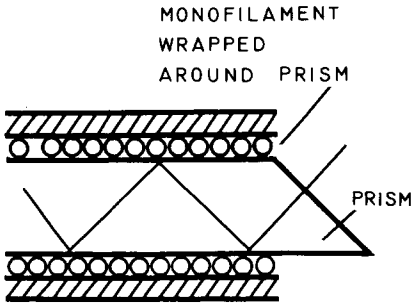

Fig. 8. Schematic diagram of geometry of fibers wrapped on ATR prism.

$$d_p = \lambda/[2\pi\eta_1(\sin^2\theta - \eta^2_{21})^{1/2}]$$

where $\eta_{21} = \eta_2/\eta_1$ is the ratio of the real part of the refractive index of the rarer medium (η_2) (generally the sample) to that of the denser material (η_1) (usually the reflection prism), θ is the angle of incidence, and λ is the wavelength. The linear dependence of the penetration depth on the wavelength leads to an enhancement of absorption bands at the longer wavelengths relative to bands of equal inherent strength at lower wavelengths. Prisms made from germanium ($\eta_1 = 4$) give both the least penetration and the least distortion of the absorption band. The disadvantage with this prism material is its transmission range of 2 to 11.5 μm or 5000 to 900 wave numbers.[28] This means that the lower range of wave numbers, 900–400 cm^{-1}, where active groups such as C—Cl, C—Si—, or epoxy rings have their absorption bands, is cut off. KRS-5 prisms have a more suitable transmission range (20,000 to 300 cm^{-1}) but their lower refractive index (2.4) gives larger penetration depths as can be seen from Table III.

Table III shows that 1% finish will contribute less than 10% to the total sampled volume even in case of a Ge prism. The possibility of determining differences in core-skin structure of PET fibers by the use of KRS-5 prism is also extremely low since the bands of interest are at low wave numbers.[29] Siblia[30] has demonstrated that coating the prism with a thin polymeric film, which does not absorb in the area of interest, will cut down the penetration depth. By using this technique, he could thus demonstrate surface enrichment of nylon in nylon-polyester biconstitutent fibers.

FTIR has the advantage of allowing subtraction of stored spectra. Although a thin surface layer will contribute very little to the total spectrum, the difference spectrum obtained with an uncoated control might allow its detection. The yarn coated with DuPont D-417 dip was used as a model yarn for optimization of experimental conditions. An IR spectrum of the cured D-417 coating is given in Figure 9(A) and of a finish free PET in Figure 9(B). A comparison shows that useful D-417 bands are at 3330, 1720, 1530, 1490, and 1205 cm^{-1}. Hartz[2] has identified some of these bands in his study. Loosely adhering spin finish components and D-417 reaction products were removed from the yarns by ultrasonic methanol cleaning since previous experiments had shown that lubricants easily smeared off onto the prism. The superior contact between the smear and the prism leads to a domination of these components in the IR spectrum. The importance of good contact between the yarn and the prism is illustrated in Figures 10(A) and 10(B). A much more intense spectrum is obtained when the ATR cell is clamped together more tightly, except for the band at around 2900 cm^{-1}. A scan of the prism afterwards showed (Fig. 11) that this band was due to a fatty acid based lubricant component present on the prism surface. A difference

TABLE III
Calculated Penetration Depths (nm) in PET Fibers with a Refractive Index of 1.64 for Germanium and KRS-5 Prisms and Different Angles of Incidence θ

Wavelength (μm)	Wave number (cm^{-1})	Penetration depths (nm)			
		Ge		KRS-5	
	θ (deg):	45	60	45	60
3	ca 3300	210	160	1095	370
5	ca. 2000	350	300	1820	620
9	ca. 1000	620	470	3280	1120

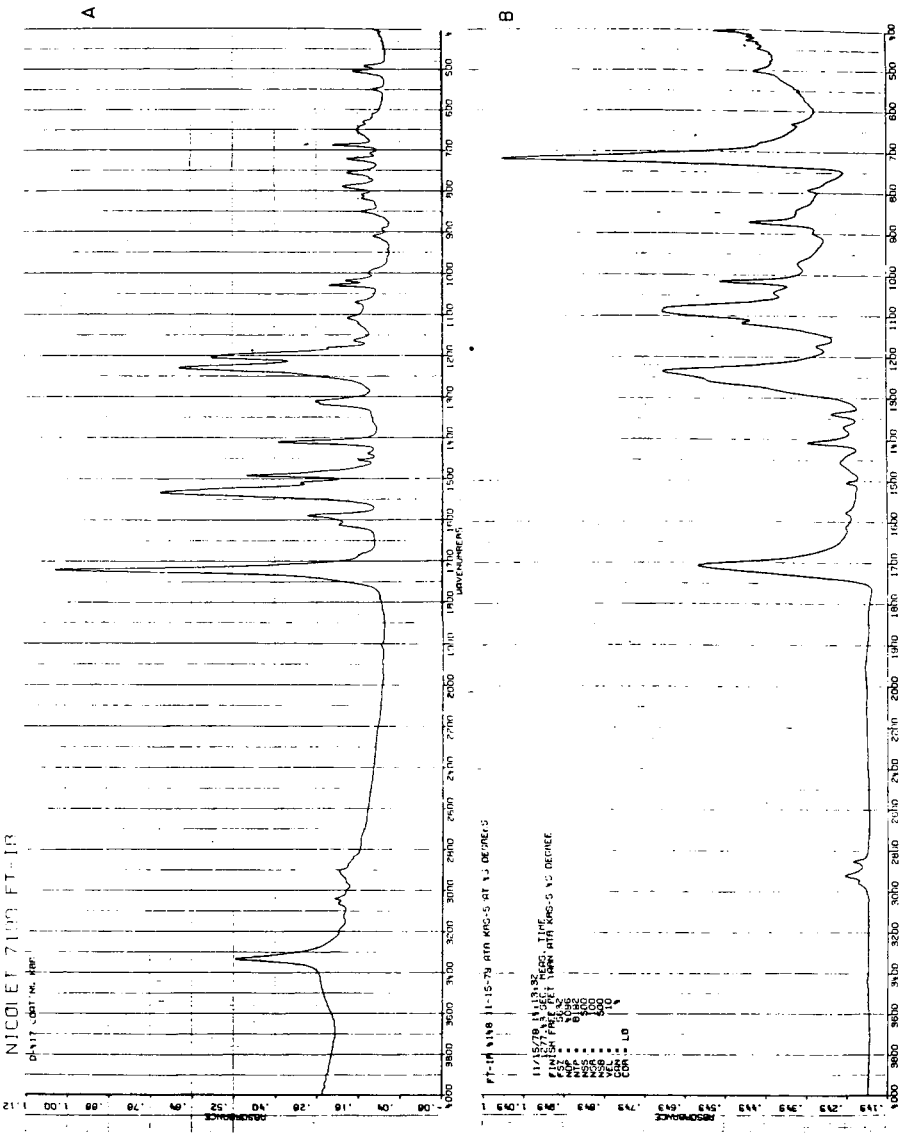

Fig. 9. (A) Transmission spectrum of cured D-417 dip. (B) Internal reflection spectrum of clean PET yarn obtained with KRS-5 prism at 45°.

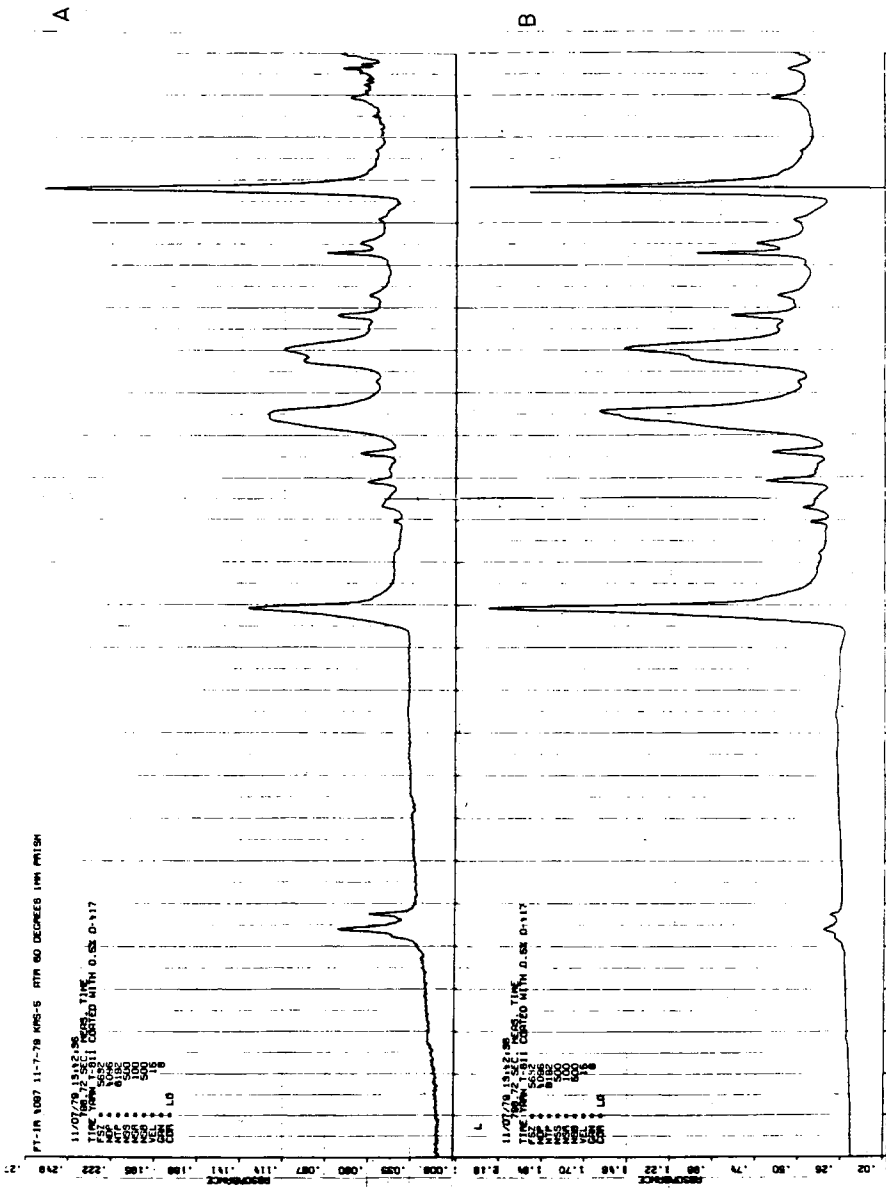

Fig. 10. Internal reflection spectrum of T-811 top-coated with D-417 dip obtained with KRS-5 prism at 60°. (A) Cell clamped together lightly. (B) Cell clamped together tightly.

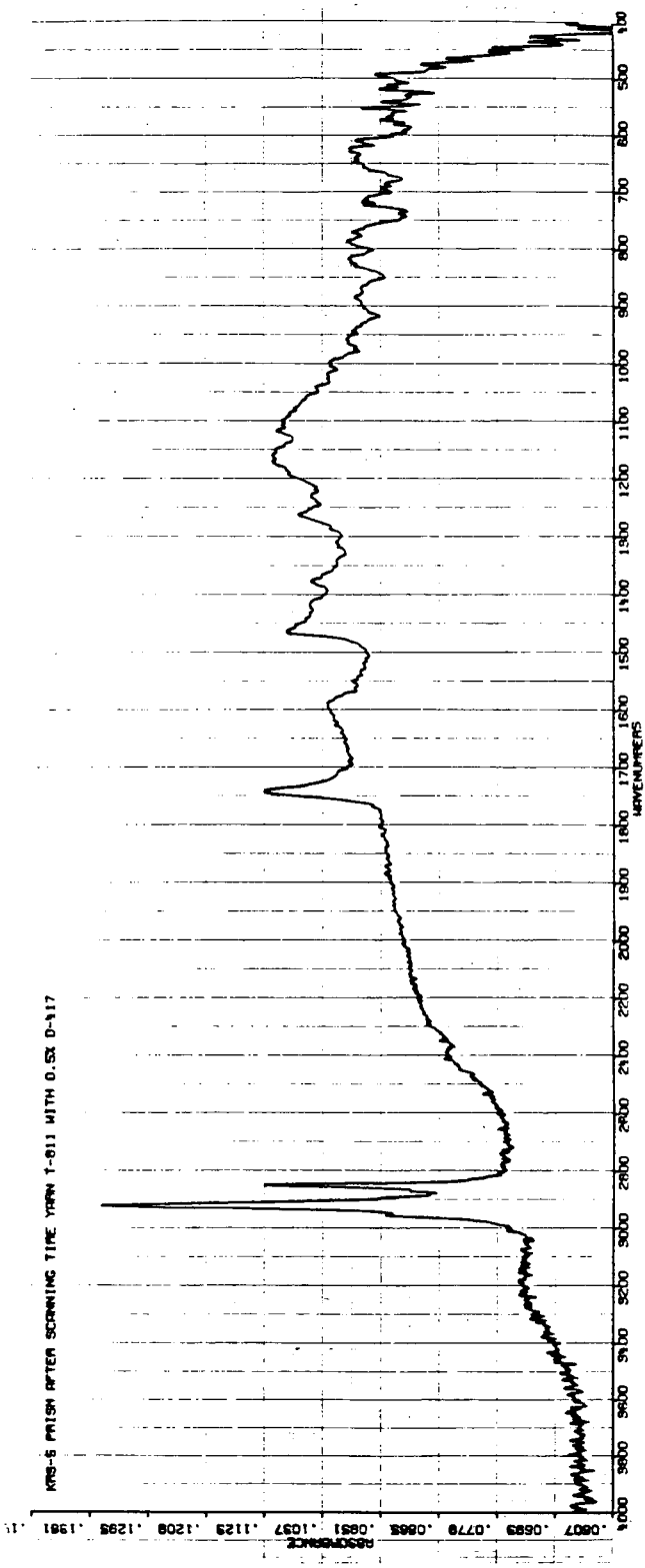

Fig. 11. Internal reflection spectrum of KRS-5 prism after yarn has been removed.

spectrum between a finish free PET tire yarn and the cleaned D-417 coated tire yarn is shown in Figure 12. This spectrum still shows PET bands and illustrates the difficulty of totally subtracting out two IR spectra obtained from different samples. Some non-PET related bands have, however, appeared at 1680, 1470, and 850. A comparison with Figure 9(A) shows that they dod not originate from the D-417 coating. Increasing the incident angle to 60° to decrease the penetration depth (Fig. 13), use of Ge as prism material (Fig. 14), and use of polarized radiation (Fig. 15) reduces the PET bands significantly. However, the dominating bands of D-417 are not observed; only those from the fatty acid lubricant are.

In order to test even higher grazing angles (80° or larger) experiments were performed in which yarn was carefully wrapped on Al foil and mounted in Wilks ATR optical system without the ATR prism. To compensate for the single reflectance signal, averaging of several thousands of scans was performed. A typical spectrum with a grazing angle of 80° is shown in Figure 16. The spectrum is a complex mixture of external and internal reflection and transmission with superimposed interference fringes. A single filament was wrapped around a graphite sheet in well separated turns in order to reduce reflectance of radiation which might pass through the fiber. The resulting spectrum (Fig. 17) shows no distinct absorption bands even after 5400 scans.

None of the FTIR techniques used showed any evidence of the D-417 coating. However, the wettability studies showed the presence of a modifying surface layer and ESCA (see below) detected both the presence of nitrogen in isocyanate residues and chlorine in glycerol epoxy residues. Neither of these methods will easily give quantitative data or the structure of species present. The much thinner films and yarns which have relatively higher concentrations of spin finish might show changes in reaction rates and thereby type of reaction products formed. Hartz[2] has shown that many finish components will interfere with the isocyanate reaction.

Further investigations with ideal model systems must, therefore, be performed to assess the possibility of using FTIR-ATR for chemical identification of thin surface layers on fibers such as PET which absorb strongly in the infrared over a wide spectral range. The ideal model system should allow deposition of nonsmearing substances at a well defined thickness in the range of 10–100 nm on a clean fiber surface.

RAMAN MICROSCOPY (MOLE)

MOLE is the acronym for microprobe molecular optics laser examiner and is, as the name implies, simultaneously a microprobe, a microscope, and a Raman microspectrophotometer.[31,32] Depending on the operation mode chosen, it is possible to record the Raman spectrum from the entire sample in the field of view of the microscope or select a small area thereof (1 μm^2). It is also possible to select a characteristic frequency for one component and thereby map the distribution of this component on the surface. Although the method utilizes the scattered radiation from the surface, considerable contribution to the resulting spectra are obtained from the bulk sample. The MOLE technique should thus have a high potential for the determination of finish distribution on fiber surfaces, especially in the case of volatile components where the high vacuum utilized in ESCA and SEM prevents their use.

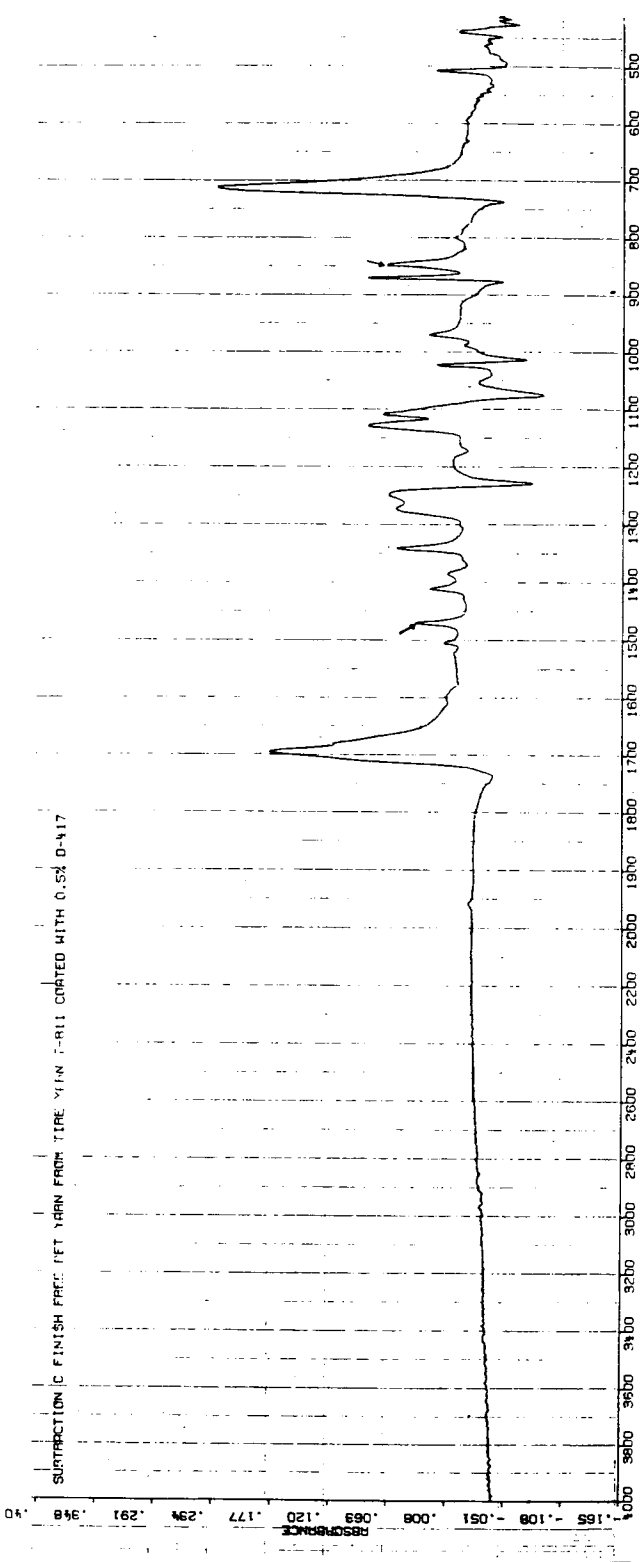

Fig. 12. Difference spectrum obtained by subtracting the internal reflection spectrum of finish free PET yarn from that of T-811 yarn topcoated with D-417. Both spectra were obtained using a KRS-5 prism at 45°.

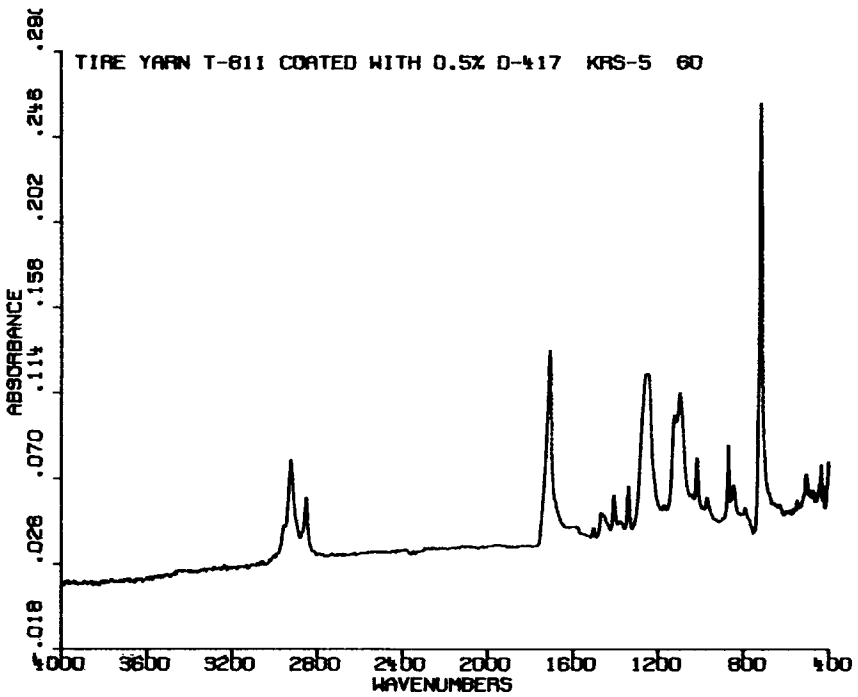

Fig. 13. Internal reflection spectrum of tire yarn T-811 top-coated with 0.5% D-417 dip obtained with a KRS-5 prism at 60°.

Preliminary investigations to determine the distribution of a finish on polyester yarn showed, however, that the finishes were too weak Raman scatteres in the presence of the much stronger polyester background. Including a strong Raman scattering functionality in the finish might help. Further development of this new microanalysis technique is necessary before it will be useful for the determination of surface films on polyester yarns.

LASER MICROPROBE MASS ANALYZER

The laser microprobe mass analyzer (LAMMA) commercial instrument that we evaluated was manufactured by Leybold-Heraeus.[33] In this instrument, a power laser is focused on a small portion of the fiber, usually around 1 μm diameter. A one-shot pulse from the laser results in volatilization of the fiber surface and simultaneous ionization of this material. A time-of-flight mass analyzer is used to characterize the ions formed. The principal advantages of this technique are the ability to obtain spatial resolution less than a fiber diameter and to control, to some extent, the depth of analysis which is generally around 0.1 μm. By using replicate analyses along the length of a fiber, it should be possible to map an element or compound along the fiber axis. Unfortunately the LAMMA appears to have limited application for our studies. As shown in Figure 18, LAMMA analysis of a surface modified PET fiber resulted in the formation of only PET degradation ions when run in the positive ion mode. The groups of ions centered at masses 63, 78, 91, 105, and 149 are those expected from

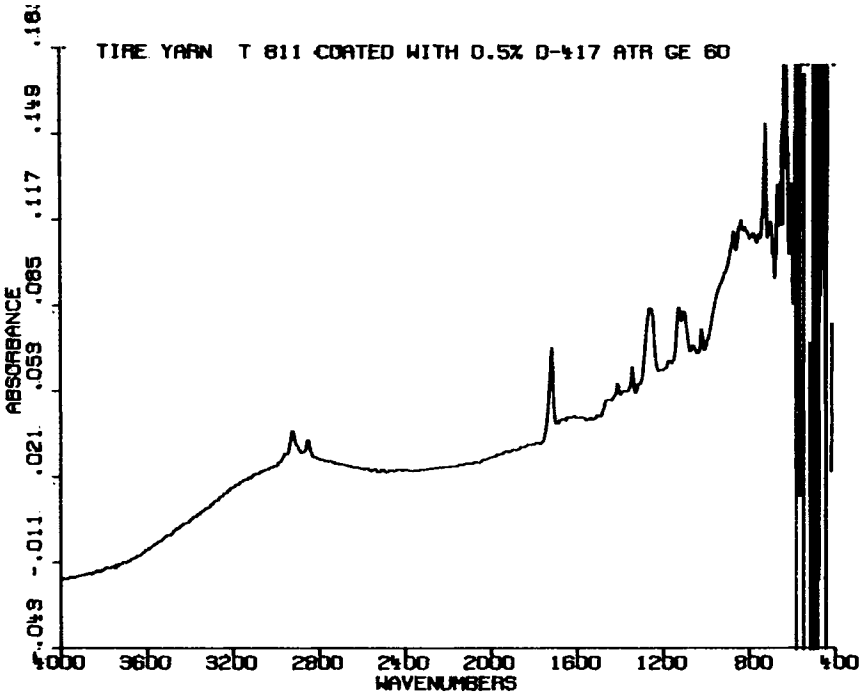

Fig. 14. Internal reflection spectrum of tire yarn T-811 top-coated with 0.5% D-417 dip obtained with a Ge prism at 60°.

a thermal pyrolysis of the polymer.[34] Although the level of detection for this technique is very low (to 10^{-19} g), no species were observed which represented the compounds used for surface modification. In the negative ion mode, even less useful information was obtained. As shown in Figure 19, the dominant species formed were C_n negative ions. These ions have been observed by other mass spectral techniques[35] and while they are of theoretical interest, they are of little practical use. In summary, it appears that the energy output of the laser is sufficient to cause disintegration of the polymer.

SECONDARY ION MASS SPECTROMETRY

In the secondary ion mass spectrometry (SIMS) analysis we find a similar situation. High energy inert gas ions bombard the fiber surface with the resultant ejection of secondary ions from the substrate. The depth of analysis by SIMS is about 10 Å (ref. 36) and hence would be desirable for this application. However, as shown in Figure 20, thermal decomposition of the fiber occurs just as it did in the LAMMA instrument, except that the aliphatic ions formed outnumber the aromatics. This is shown by the aliphatic groups 39 to 45 and 56 to 58 versus the aromatic group 50 to 53. In the case of SIMS, degradation or pyrolysis is very severe and the technique offers less promise than the LAMMA.

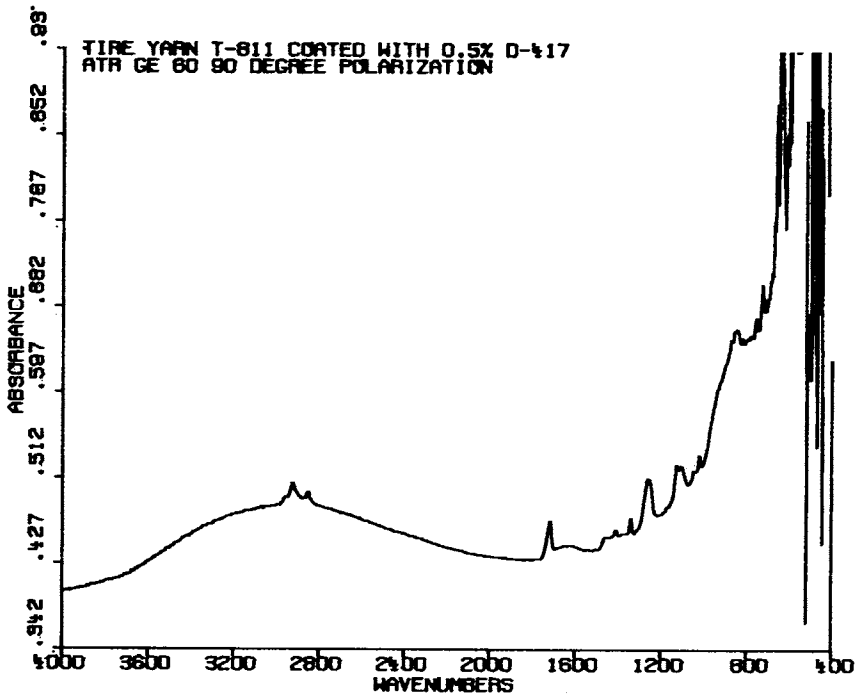

Fig. 15. Internal reflection spectrum of tire yarn T-811 top-coated with 0.5% D-417 dip obtained with a Ge prism at 60° and with 90° polarization.

ELECTRON SPECTROSCOPY FOR CHEMICAL ANALYSIS

Of the five spectroscopic techniques studied, electron spectroscopy for chemical analysis (ESCA) offers the greatest promise for elucidating the mechanisms of surface modification. With a sampling depth of roughtly 50 Å (ref. 37) the ESCA is suitable for fiber surface analysis. Most elements used in these fiber systems can be detected by ESCA and many of them, such as carbon, nitrogen, and oxygen, show changes in binding energy with change in oxidation state. The technique is useful then for chemical as well as elemental analysis of fiber surfaces. In addition, the x-ray beam does not cause significant degradation of the samples, although some discoloration of the fibers does occur.

Excellent overviews illustrating the power of ESCA for studying polymer surfaces are given in Ref. 38 and 39. Examples of ESCA applications in fiber analysis include the characterization of wool fibers[40] and graphite fibers.[41] Various techniques have been developed for determining the thickness of coatings on polymer films, such as variation in take-off angle,[37] but these are not generally applicable to the analysis of fiber bundles because of their geometry. Although distribution and thickness of surface modifiers on fibers is an ultimate goal, some things can be learned by an examination of more ideal film surfaces.

For example, consider the D-417 system on PET film. This system is the reaction product of a blocked diisocyanate and a glycerol epoxy which contains chlorine. Nitrogen can thus be used as a tag for measuring the amount of isocyanate reaction products on the surface while chlorine is a tag for glycerol epoxy. ESCA was used to measure the relative amounts of N and Cl on prepared films and T-811 yarn and some differences are found. Table IV shows the relative

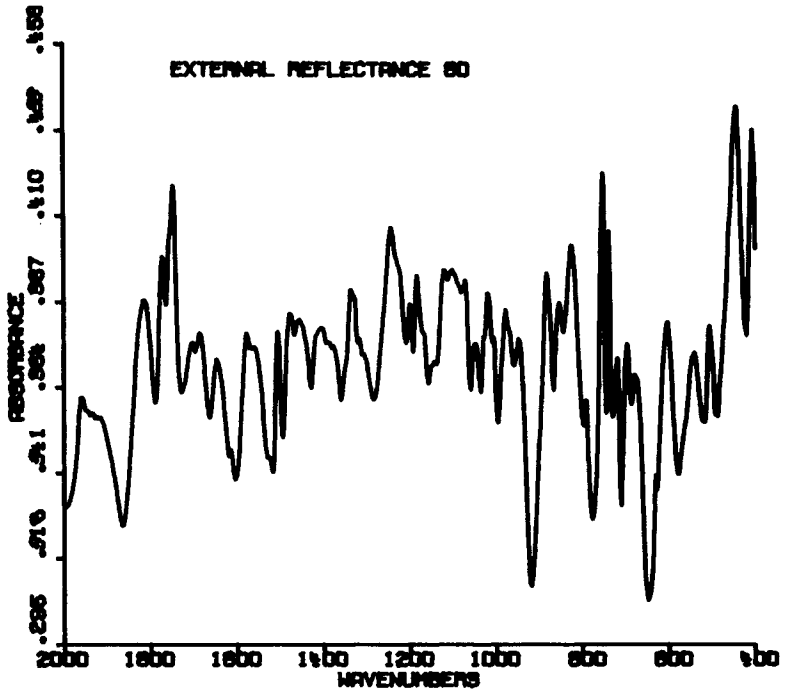

Fig. 16. "External" reflection spectrum of tire yarn T-811 top-coated with 0.5% D-417, dip at a grazing angle of 80°.

TABLE IV
Ratios of ESCA Peak Heights in PET Samples; Data are Uncorrected for Instrument Response Factors

	Nitrogen/chlorine ratio
D-417 treated film	1.8
D-417 treated film, cleaned	1.9
D-417 top-coated T-811 yarn, cleaned	0.8
D-417 top-coated T-800 yarn	1.0
D-417 top-coated T-800 yarn, cleaned	1.6

peak heights of the nitrogen and chlorine bands. Corrections have not been made for the response factors of these two elements and thus these figures do not represent relative amounts on a molar basis. The D-417 coated and heat treated PET film has a N/Cl ratio of about 1.8 both before and after cleaning with methanol. Both glycerol epoxy and isocyanate reaction products are extractable, and can be removed to the same extent. However, for a cleaned T-811 yarn the N/Cl ratio is 0.8, for the topcoated T-800 yarn 1.0 and after cleaning this yarn 1.6. The unblocking reaction of the blocked diisocyanate is sensitive to various types of finish components[2] and special tire yarn finishes have been developed for use with D-417 dip. The T-811 finish has been developed to give an optimal adhesive activated yarn which bonds directly to RFL. It is thus not optimized for the D-417 systems so the N/Cl ratio has less significance for this type of yarn. The T-800 yarn used for the topcoating experiment has the same finish as that on the yarns used for the D-417 cord treatments. The finish of the T-800 yarn

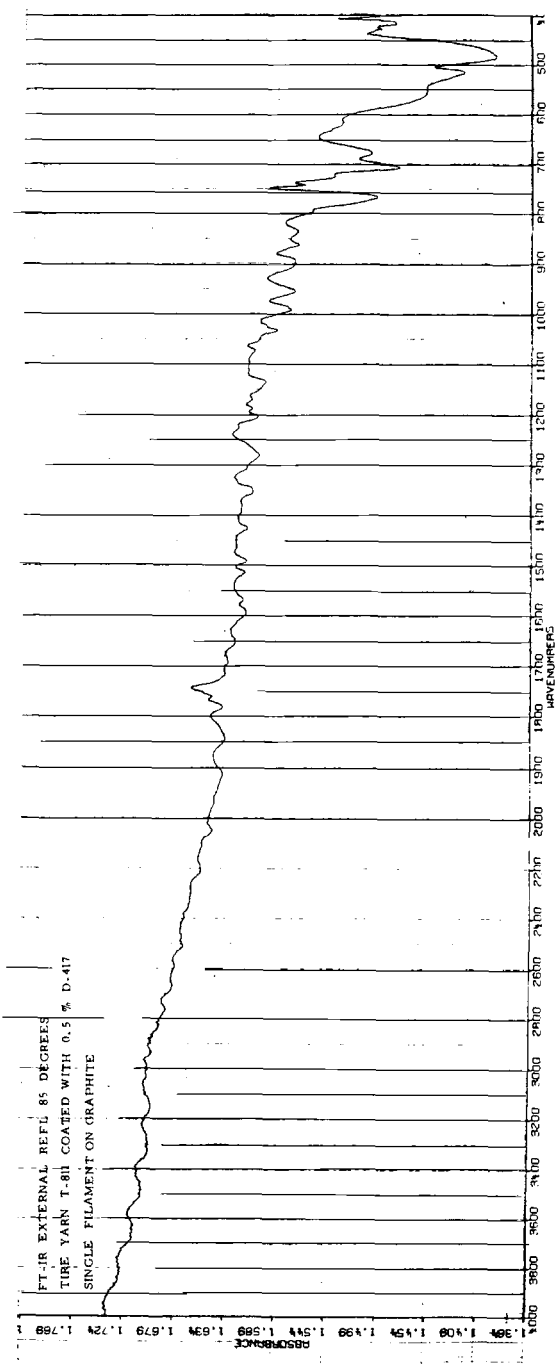

Fig. 17. "External" reflection spectrum of a single fiber of tire yarn T-811 coated with 0.5% D-417, wrapped around graphite, obtained at 85° grazing angle.

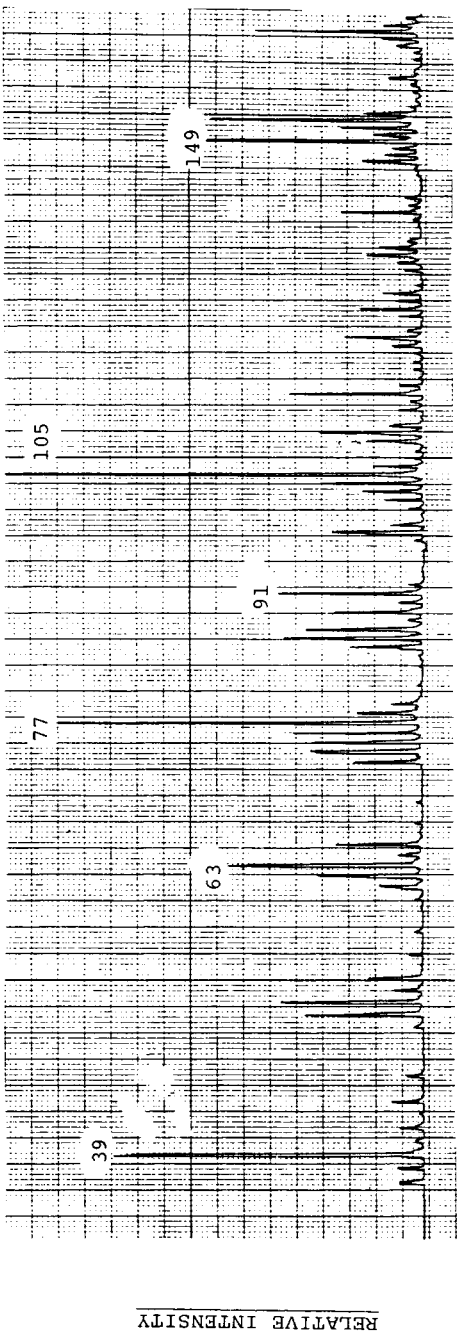

Fig. 18. LAMMA spectrum of a surface modified PET yarn: positive ion mode.

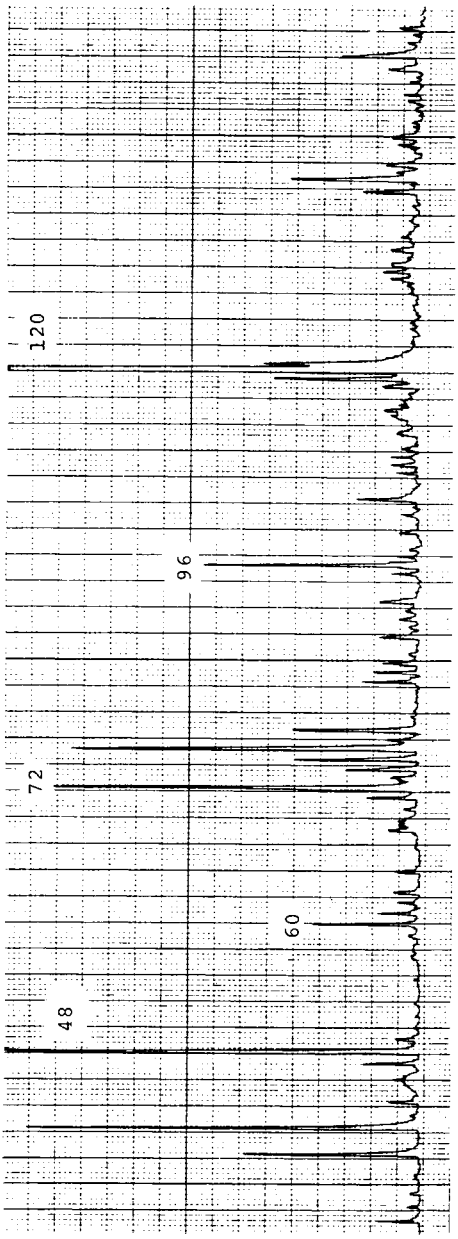

Fig. 19. LAMMA spectrum of a surface modified PET yarn: negative ion mode.

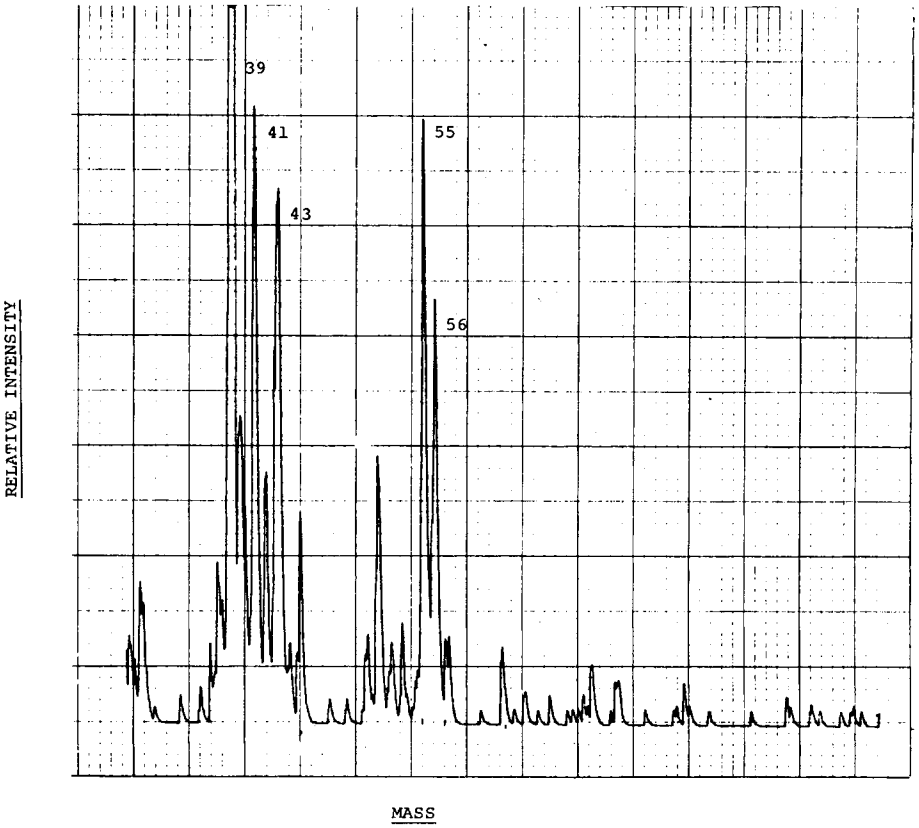

Fig. 20. SIMS spectrum of a surface modified PET yarn: positive ion mode.

will accordingly not chemically interfere with the desired reactions of the D-417 system. Since the only source of Cl is the glycerol epoxy, the lower ratio (1.0) for as-spun T-800 yarn compared to the films indicates a net loss of nitrogen. Apparently, some of the unblocked isocyanate does not react to form the desired polyurethane. A possible side reaction is that of the isocyanate with trace water to form urea, which in turn can heat degrade and release ammonia, thereby lowering the nitrogen content. The comparatively higher dilution of the D-417 with finish when topcoated on yarn would increase the likelihood of unwanted side reactions. The cleaned T-800 yarn shows a N/Cl ratio of 1.6, i.e. almost the same as for the film sample. Therefore, the surface bonded reaction products of the D-417 system on the T-800 yarn seem to be the desired polyurethane.

Depth profiling of surface modifiers is of interest but problems arise when using an ion beam to remove outer layers of the fiber surface. For example, most of the carbon is reduced by argon ion etching, as shown in Figure 21. Prior to etching, the various types of carbon can be clearly distinguished: the aromatics, the epoxy carbons, and the carboxyls. After etching, there is basically only one form of carbon remaining, and that is a reduced form. The other problems which arise with etching are as follows: (i) To what extent are surface species not sputtered from the surface but rather imbedded into the polymer by the ion beam?; and (ii) what is the rate of removal of polymeric material by the sputtering

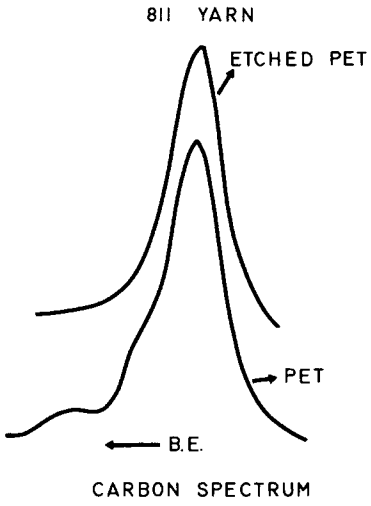

Fig. 21. Carbon ESCA spectra of PET fiber before and after argon ion etching.

beam? At this point we do not have a clear understanding of the extent of scrambling on the polymer surface but it is hoped that SEM and ESCA on model systems will aid in this problem.

Figure 22 shows the carbon spectrum of a PET film covered with 100 Å of vapor deposited gold/palladium alloy. The unetched sample shows two large peaks. The higher binding energy band is believed to arise from an interaction between the photoejected carbon electrons and the gold substrate. The lower binding energy band represents those electrons which escape freely. After a 3 min etch, the carbon signal has increased by nearly 100%, and after 5 min, the carbon signal reaches a maximum. This means that effectively all of the gold alloy is removed in a 5 min etch so that the etch rate is approximately 20 Å/min. However, fluorescence detection of gold in an SEM shows Au to be present evenly in the sample and thus some imbedding of Au in the PET has occurred.

We can reasonably expect that the etching rate of polymeric organic material would be different from that of a metallic material.

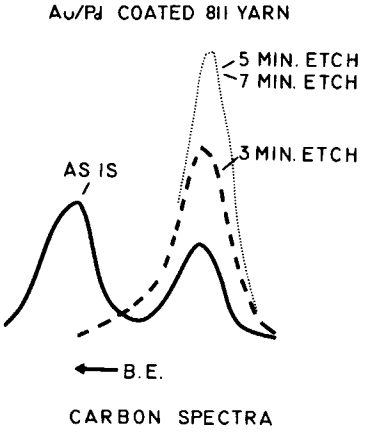

Fig. 22. Carbon ESCA spectra of PET fiber coated with 100 Å of Au/Pd alloy. Intensity of carbon peak illustrates the rate of removal of the metal layer.

As discussed previously, the geometry of fibers and fiber bundles can create problems. As shown in Figure 23, the curvature of a single strand causes some confusion in defining sampling depth. With the entrance to the analyzer in the direction of the top of the diagram, we can define the sampling depth (D) as being equivalent to the escape depth (λ). For an atom B at the edge of the fiber, the sampling depth is much less for a given escape depth. The effective sampling depth thus varies depending on the position on the fiber curve.

In etching, one should be careful to ensure that the angle of the sample to the argon beam is the same as the take-off angle to the analyzer. If this precaution is not taken, the analyzed area will not in fact be etched. As a final point, one must consider the possibility of puddles forming between individual fiber strands which would lead to apparent and erroneously high levels of surface species.

CONCLUSIONS

The investigations performed show that wettability studies according to the Wilhelmy method can give indications of the degree and distribution of a surface modification and also information concerning its permanence. SEM studies can mainly prove the existence of uneven layers on the microscopic scale. The presence of a continuous thin film is difficult to assess with this technique. Spectroscopic methods which will determine the chemical nature of surfaces are necessary for identification of these thin films as well as other forms of surface modification. The spectroscopic method which shows greatest promise is ESCA. Its principle application is in the determination of relative amounts of surface elements, as shown in the D-417 system. ESCA may not yield quite as much definitive information on structural groups as does infrared, but its surface sensitivity is an important trade-off. The LAMMA and SIMS techniques appear to be too destructive for these applications.

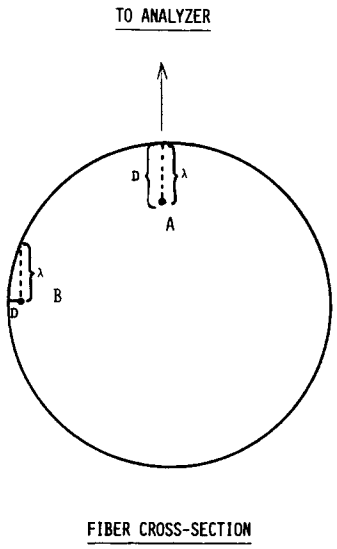

Fig. 23. Diagrammatic representation of a fiber strand illustrating changes in sampling depth for atoms at different positions within the fiber. For a given escape depth λ, the actual sampling depth is greatly reduced for atoms at the side of the fiber.

The investigations suggest that yarns topcoated with D-417 dip have an uneven surface coating of the formed polyurethane and that the desired polyurethane reaction is not the only one taking place on the PET yarns. A much lower surface concentration of D-417 will be obtained on a yarn than on a cord because of the much larger yarn fiber surface area compared with that of the cord. There is also a higher dilution of D-417 reagents by the finish in the case of topcoated yarn. The lower adhesion level observed for D-417 topcoated yarn as compared to a coated cord can thus be ascribed to the cord geometry offering a better outer surface coverage than the yarn at the same level of D-417 dip.

Valuable comments from A. DiEdwardo, Dr. G. Hardy, and Dr. R. M. Mininni are highly appreciated. Dr. R. Kemmerer, Professor D. M. Hercules, Dr. J. Mather, and Mrs. L. Sawyer are acknowledged for performing the FTIR, the SIMS and LAMMA, and the MOLE and SEM experiments. Miss A. Kravas, K. Damerau, and D. Van Duyne are acknowledged for their valuable assistance in wetting and ESCA experiments.

References

1. M. J. Schick, Ed., *Surface Characteristics of Fibers and Textiles*, Marcel Dekker, New York, 1975, Parts I and II.
2. R. E. Hartz, *J. Appl. Polym. Sci.*, **19,** 735 (1975).
3. H. R. Billica and R. D. van Veld, in ref. 1, Part I, Chap. 7.
4. V. Peck, *J. Appl. Polym. Sci. Appl. Polym. Symp.*, **16,** 19 (1972).
5. B. W. Davis, *J. Colloid Interface Sci.*, **59,** 420 (1977).
6. S. Wu, *J. Macromol. Sci. Rev. Macromol. Chem.*, **C10,** 1 (1974).
7. R. J. Good and L. A. Girifalco, *J. Phys. Chem.*, **64,** 561 (1960).
8. R. J. Good, in *Surface and Colloid Science*, R. J. Good and R. R. Stromberg, Eds., Plenum, New York, 1979, Vol. 11, Chap. 1.
9. F. M. Fowkes, *J. Phys. Chem.*, **67,** 2538 (1963).
10. D. K. Owens, and R. C. Wendt, *J. Appl. Polym. Sci.*, **13,** 1741 (1969).
11. D. H. Kaelble and K. C. Uy, *J. Adhes.*, **2,** 50 (1970).
12. D. H. Kaelble, *J. Adhes.*, **2,** 66 (1970).
13. S. Wu, *J. Adhes.*, **5,** 39 (1973).
14. S. Wu, *J. Polym. Sci., Part C*, **34,** 19 (1971).
15. F. M. Fowkes and M. A. Mostaja, *Ind. Eng. Chem. Prod. Res. Div.*, **17,** 3 (1978).
16. F. M. Fowkes, in *Adhesion and Adsorption of Polymers*, L. H. Lee, Ed, Plenum, New York, 1980, Part A, p. 43.
17. F. M. Fowkes, Air Force Office of Scientific Research Report No. AFOSR-TR-80-0066, 1979, p. 20.
18. R. E. Johnson, Jr. and R. H. Dettre, in *Surface and Colloid Science*, E. Matejevic, Ed., Wiley-Interscience, New York, 1969, Vol. 2, Chap. 2.
19. T. Smith and G. Lindberg, *J. Colloid Interface Sci.*, **66,** 363 (1978).
20. B. Miller, in ref. 1, Part II, Chap. 11.
21. A. W. Neuman and W. Tanner, *Proc. 5th Int. Cong. Surf. Activity*, **2,** 727 (1968).
22. G. E. P. Elliott and A. C. Riddiford, *J. Colloid Interface Sci.*, **23,** 389 (1967).
23. G. Inverarity, *Br. Polym. J.*, **1,** 245 (1969).
24. H. A. Willis, and V. J. Zichy, in *Polymer Surfaces*, D. T. Clark and W. J. Feast, Eds., Wiley, New York, 1978, Chap. 15.
25. G. W. Urbanczyk, *J. Polym. Sci. Polym. Symp.*, **58,** 311 (1977).
26. D. J. Carlsson, T. Suprunchuk, and D. M. Wills, *Can. Tex. J.*, **87** (11), 73 (1970).
27. V. Krentz, *Milliand Text., Ger.*, **5,** 557 (1969).
28. J. P. Siblia, in ref 1, Part I, Chap. 8.
29. W. O. Statton, J. L. Koenig, and M. Hannon, *J. Appl. Phys.* **41,** 4290 (1970).
30. J. P. Siblia, *J. Appl. Polym. Sci.*, **17,** 2911 (1973).
31. M. Delhaye, M. Leclercq, and D. Landon, *Ind. Res.*, **19,** 69 (1977).
32. P. Dhamelincourt, F. Wallart, M. Leclercq, A. T. N'Guyen, and D. O. Landon, *Anal. Chem.*, **51,** 414A (1979).
33. Inficon Leybold Heraeus, Inc., 6500 Fly Road, East Syracuse, N.Y. 13057.

34. I. Luderwald and H. Urrutia, in *Analytical Pyrolysis*, C. E. Roland and Carol A. Cramer, Eds., Elsevier, New York, 1977, p. 139.

35. T. Keough, Ph.D. thesis, Purdue University, 1975.

36. G. K. Wehner, in *Methods of Surface Analysis*, C. W. Czanderna, Ed., Elsevier, Amsterdam, 1975, Chap. 1.

37. W. M. Riggs and M. J. Parker in ref. 36, Chap. 4.

38. D. T. Clark, in *Polymer Surfaces*, D. T. Clark and W. J. Feast, Eds., Wiley, New York, 1978, p. 309.

39. D. T. Clark, in *Characterization of Metal and Polymer Surfaces*, L. H. Lee, Ed., Academic, London, 1977, p. 5.

40. M. M. Millard, in ref. 39, p. 86.

41. D. M. Brewis, J. Comyn, J. R. Fowler D. Briggs, and V. A. Gibson, *Fiber Sci. Technol.*, **12**(1), 41 (1979).

Received December 5, 1980
Accepted January 19, 1981